

# Relativistic descriptions of final-state interactions in charged-current quasielastic antineutrino-nucleus scattering at MiniBooNE kinematics.

Andrea Meucci and Carlotta Giusti

*Dipartimento di Fisica Nucleare e Teorica, Università degli Studi di Pavia and INFN, Sezione di Pavia, via A. Bassi 6, I-27100 Pavia, Italy*

(Dated: May 14, 2022)

The analysis of the recent charged-current neutrino-nucleus scattering cross sections measured by the MiniBooNE Collaboration requires relativistic theoretical descriptions also accounting for the role of final-state interactions. In this work, we evaluate differential antineutrino-nucleus cross sections with the relativistic Green's function model, where the final-state interactions are described in the inclusive scattering consistently with the exclusive scattering using a complex optical potential. The sensitivity to the parameterization adopted for the phenomenological optical potential is discussed. The predictions of the relativistic Green's function model are compared with the results of different descriptions of final-state interactions.

PACS numbers: 25.30.Pt; 13.15.+g; 24.10.Jv

Keywords: Neutrino scattering; Neutrino-induced reactions; Relativistic models

## I. INTRODUCTION

The MiniBooNE Collaboration has recently reported [1] a measurement of the charged-current quasielastic (CCQE) flux-averaged double-differential muon neutrino cross section on  $^{12}\text{C}$  in an energy range up to  $\approx 3$  GeV. The neutrino-nucleus CCQE reaction in MiniBooNE may be considered as scattering of an incident neutrino with a single nucleon bound in carbon, but it can also be sensitive to contributions from collective nuclear effects, whose clear understanding is crucial for the analysis of ongoing and future neutrino oscillation measurements [1–7].

When a dipole dependence on the four-momentum transferred squared  $Q^2$  is assumed for the axial form factor, the nucleon axial mass  $M_A$  has been used as a free parameter within the relativistic Fermi gas (RFG) model [8, 9]. Recent CCQE measurements [3, 4] reported values of  $M_A \approx 1.2$  GeV/ $c^2$ , significantly larger than the world average value from the deuterium data of  $M_A = 1.03$  GeV/ $c^2$  [10, 11]. In agreement with these results, the MiniBooNE collaboration reported values of  $M_A = 1.35 \pm 0.17$  GeV/ $c^2$  for the CCQE measurements [1] and  $M_A = 1.39 \pm 0.11$  GeV/ $c^2$  for the neutral-current elastic (NCE) data [2]. A recent application of analyticity and dispersion relations to the axial vector form factor to find constraints for the axial mass parameter using the CCQE data from MiniBooNE is presented in Ref. [12] and produces a value of  $M_A = 0.85^{+0.22}_{-0.07} \pm 0.09$  GeV, which significantly differs from the RFG extraction.

The energy region considered in the MiniBooNE experiments, with neutrino and antineutrino energy up to  $\approx 3$  GeV and average energy of the muon neutrino (antineutrino) flux  $\approx 0.79$  (0.66) GeV [13], requires the use of a relativistic model, where not only relativistic kinematics should be considered, but also nuclear dynamics and current operators should be described within a relativistic framework. From the comparison with electron scattering data it is known that the RFG, although able

of getting the basic shape and size of the response, turns out to be a too naive model to correctly account for important details of the nuclear dynamics. Thus, the larger axial mass needed by the RFG could be considered as an effective value to incorporate nuclear effects into the calculation rather than a clear signal of a modified axial mass.

At intermediate energy, quasielastic (QE) electron scattering calculations [14, 15], which were able to successfully describe a wide number of experimental data, can provide a useful tool to study neutrino-induced processes. Several theoretical models have been applied in recent years to  $\nu$ -nucleus scattering reactions and some of them have been compared with the MiniBooNE data, both in the CCQE and in the NCE channels. At the level of the impulse approximation (IA), models based on the use of a realistic spectral function [16, 17], which are built within a nonrelativistic framework, underestimate the experimental CCQE and NCE cross sections unless  $M_A$  is enlarged with respect to the world average value. The same results are obtained by models based on the relativistic IA (RIA) [18–20]. However, the reaction may have significant contributions from effects beyond the IA in some kinematic regions where the experimental neutrino flux has significant strength. For instance, in the models of Refs. [21–25] the contribution of multinucleon excitations to CCQE scattering has been found sizable and able to bring the theory in agreement with the experimental MiniBooNE cross sections without increasing the value of  $M_A$ .

The role of processes involving two-body currents compared to the IA models has been discussed in Refs. [17, 26–28]. A careful evaluation of all nuclear effects and of the relevance of multinucleon emission and of some non-nucleonic contributions [29–32] would be interesting for a deeper understanding of the reaction dynamic. However, fully relativistic microscopic calculations of two-particle-two-hole (2p-2h) contributions are extremely difficult and may be bound to model dependent assumptions. For

instance, the part of the 2p-2h excitations which may be reached through two-body meson-exchange currents (MEC), in particular the contribution of the vector MEC in the 2p-2h sector, evaluated in the model of Ref. [33], has been incorporated in a phenomenological approach based on the superscaling behavior of electron scattering data [26, 27, 34]. The effects of MEC are important relative to the QE contribution, especially for the antineutrino cross section, where the destructive vector-axial interference term reduces the pure QE contribution and the MEC have a more significant role [34].

Within the QE kinematic domain, the treatment of the final-state interactions (FSI) between the ejected nucleon and the residual nucleus is an essential ingredient for the comparison with data. The relevance of FSI has been clearly stated in the case of exclusive ( $e, e'p$ ) processes, where the use of complex optical potentials in the distorted wave impulse approximation (DWIA) is required [14, 15, 35–41]. However, the pure DWIA approach, which is based on the use of an absorptive complex potential, would be inconsistent in the analysis of inclusive scattering, where all final-state channels should be retained and the total flux, although redistributed among all possible channels due to FSI, must be conserved. Different approaches have been used to describe FSI in relativistic calculations for the inclusive QE electron- and neutrino-nucleus scattering [42–52]. In the relativistic plane-wave impulse approximation (RPWIA), FSI are simply neglected. In another approach, FSI are included in DWIA calculations where the final nucleon state is evaluated with real potentials, either retaining only the real part of the relativistic energy-dependent complex optical potential (rROP), or using the same relativistic mean field potential considered in describing the initial nucleon state (RMF). Although conserving the flux, the rROP is unsatisfactory from a theoretical point of view, since it relies on an energy-dependent potential, which reflects the different contribution of open inelastic channels for each energy, and under such conditions dispersion relations dictate that the potential should have a nonzero imaginary term [53]. On the other hand, in the RMF model the same strong energy-independent real potential is used for both bound and scattering states. It fulfills the dispersion relations [53] and also the continuity equation.

In a different description of FSI relativistic Green's function (RGF) techniques [45, 46, 51, 52, 54, 55] are used. In the RGF model, under suitable approximations, which are basically related to the impulse approximation, the components of the hadron tensor are written in terms of the single particle optical model Green's function, whose self-energy is the Feshbach optical potential. The explicit calculation of the single particle Green's function can be avoided by its spectral representation, which is based on a biorthogonal expansion in terms of a non Hermitian optical potential  $\mathcal{H}$  and of its Hermitian conjugate  $\mathcal{H}^\dagger$ . Calculations require matrix elements of the same type as the DWIA ones for the case of

exclusive ( $e, e'p$ ) processes in Ref. [37], but involve eigenfunctions of both  $\mathcal{H}$  and  $\mathcal{H}^\dagger$ , where the imaginary part gives in one case an absorption and in the other case a gain of flux. This formalism allows us to reconstruct the flux lost into nonelastic channels in the case of the inclusive response starting from the complex optical potential which describes elastic nucleon-nucleus scattering data. Thus, it provides a consistent treatment of FSI in the exclusive and in the inclusive scattering and gives a good description of ( $e, e'$ ) data [46, 51]. Due to the analyticity properties of the optical potential, the RGF model fulfills the Coulomb sum rule [46, 53, 54]. In addition, the RMF and RGF reproduce also the behavior of the scaling function extracted from the electron scattering data [51].

These different descriptions of FSI have been compared in [51] for the inclusive QE electron scattering, in Ref. [52] for the CCQE neutrino scattering, and in Refs. [56, 57] with the CCQE and NCE MiniBooNE data. In Ref. [56] both the RMF and the RGF give a good description of the shape of the CCQE experimental data and, moreover, the RGF can give cross sections of the same magnitude as the experimental ones without the need to increase the value of  $M_A$ . Similar results are obtained in Ref. [57], where the RGF results and their interpretation in comparison with the NCE data from MiniBooNE are discussed.

In this paper different relativistic descriptions of FSI for CCQE  $\bar{\nu}$ -nucleus reactions are discussed and results for the double-differential cross section averaged over the  $\bar{\nu}_\mu$  MiniBooNE flux are presented. The MiniBooNE collaboration has accumulated an extensive data set of  $\nu_\mu$  events, but it has also measured  $\bar{\nu}_\mu$  CCQE events. The analysis of the antineutrino data is currently ongoing [58] and some preliminary results can be found in the MiniBooNE website [59]. When available, the antineutrino measurements will be an additional source of information about the weak charged-current lepton-nucleus interaction and, combined with the corresponding neutrino data, will provide important insight about the role of the longitudinal, transverse, and interference vector-axial responses which enter the cross sections. Indeed, being aware of the interpretative questions which may be connected to the fact that the neutrino and the antineutrino fluxes at MiniBooNE are different, with the  $\bar{\nu}_\mu$  flux significantly smaller and with lower average energy than the  $\nu_\mu$  one, measurements of both reactions would be useful to clarify the role of nuclear effects in the analysis of lepton-nucleus processes.

## II. RESULTS AND DISCUSSION

In all the calculations presented in this work the bound nucleon states are taken as self-consistent Dirac-Hartree solutions derived within a relativistic mean field approach using a Lagrangian containing  $\sigma$ ,  $\omega$ , and  $\rho$  mesons [60–62]. In the RGF calculations we have used two parameterizations for the relativistic optical poten-

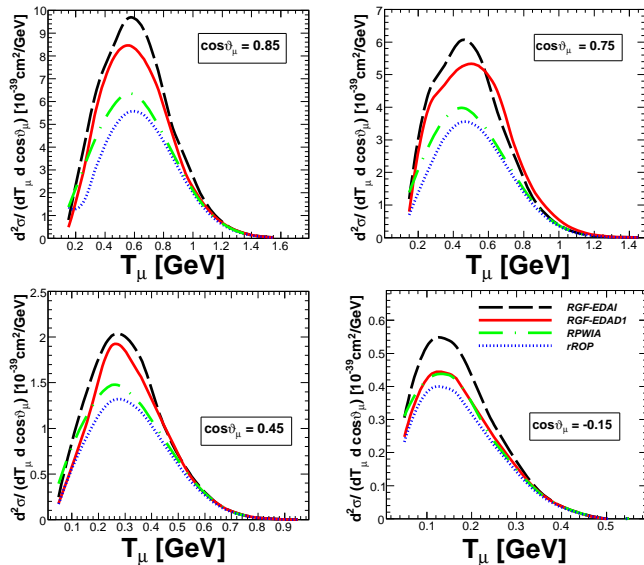


Figure 1. (color online) Flux-averaged double-differential cross section per target nucleon for the CCQE  $^{12}\text{C}(\bar{\nu}_\mu, \mu^+)$  reaction as a function of  $T_\mu$  for four angular bins of  $\cos\vartheta_\mu$  calculated with the RGF-EDAD1 (solid lines) and the RGF-EDAI (dashed lines). The dotted lines are the rROP results calculated with the EDAI potential and the dot-dashed lines are the RPWIA results.

tial: the Energy-Dependent but A-Independent EDAI (where the  $A$  represents the atomic number) and the Energy-Dependent and A-Dependent EDAD1 complex phenomenological potentials of Refs. [63–65], which are fitted to elastic proton scattering data in an energy range up to 1040 MeV. We note that whereas EDAD1 is a global parameterization, EDAI is a single-nucleus parameterization, which is constructed to fit scattering data just on  $^{12}\text{C}$  and, as such, does have an edge in terms of better reproduction of the elastic proton- $^{12}\text{C}$  phenomenology [63] compared to EDAD1, and also leads to a better description of the inclusive quasielastic ( $e, e'$ ) cross sections, as well as to CCQE and NCE results in better agreement with the MiniBooNE data [56, 57].

In Fig. 1 the CCQE double-differential  $^{12}\text{C}(\bar{\nu}_\mu, \mu^+)$  cross section per target nucleon integrated over the MiniBooNE  $\bar{\nu}_\mu$  flux is shown as a function of the muon kinetic energy  $T_\mu$  for four angular bins of  $\cos\vartheta_\mu$ , where  $\vartheta_\mu$  is the muon scattering angle, ranging from forward to backward angles. In the RPWIA calculations FSI are completely neglected. The rROP results, where calculations are performed with a pure real optical potential, are usually 15% lower than the RPWIA ones. The rROP generally underestimates the  $\nu$  experimental data unless a larger axial mass, e.g.,  $M_A \approx 1.3 - 1.4 \text{ GeV}/c^2$ , is used. However, independently of its comparison with the data, the rROP model, which is based on an energy-dependent potential, has important physical drawbacks [46, 52, 53, 56]. The RGF cross sections with both optical potentials are

larger than the RPWIA and the rROP ones. The differences between the RGF results with the two optical potentials are clearly visible. For instance, the EDAI and EDAD1 potentials yield differences by about 15%–20% to the cross section in the peak region for the forward angle scattering bins  $\cos\vartheta_\mu = 0.85, 0.75$ . Somewhat closer predictions are obtained in the bin  $\cos\vartheta_\mu = 0.45$ , while for the backward angular bin  $\cos\vartheta_\mu = -0.15$  the differences are enhanced up to 25%, but the magnitude of the cross sections is significantly reduced. We note that the relative differences between the RGF results with the two optical potentials are somewhat larger in neutrino scattering [56]. The different behavior of the RGF in neutrino and antineutrino scattering is related to the relative strength of the vector-axial response, which is constructive in  $\nu$  scattering and destructive in  $\bar{\nu}$  scattering with respect to the longitudinal and transverse ones [52]. Moreover, the differences between the neutrino and antineutrino MiniBooNE fluxes, make the comparison between the results of  $\nu_\mu$ -nucleus and  $\bar{\nu}_\mu$ -nucleus scattering not straightforward.

The comparison between the RGF results obtained with the EDAI and EDAD1 potentials can give an idea of how the predictions of the model are affected by uncertainties in the determination of the phenomenological optical potential. The differences depend on the energy and momentum transfer and are essentially due to the different values of the imaginary parts of the two potentials, which account for the overall effects of inelastic channels and are not univocally determined from the elastic phenomenology. In contrast, the real terms are very similar for different parameterizations and give very similar results. In the rROP calculation shown in Fig. 1, the real part of the EDAI potential has been used, but a calculation with EDAD1 would give in practice the same result. The results in Fig. 1 stress the importance of FSI and, in particular, of the imaginary part of the relativistic optical potential, which plays a different role in the different approaches. In the rROP, the imaginary part is neglected and the total flux is automatically conserved. The RGF results presented here contain the contribution of both terms of the hadron tensor in Eq. (61) of Ref. [46]. The calculation of the second term, which is entirely due to the imaginary part of the optical potential, is a hard and time consuming numerical task which requires the integration over all the eigenfunctions of the continuum spectrum of the optical potential. Numerical uncertainties on this term are anyhow under control and, from many calculations in different kinematics, have been estimated at most within 10%. In the RGF, the imaginary part redistributes the flux in all the final-state channels and, in each channel, the loss of flux towards other inelastic channels (either multinucleon emission or non-nucleonic excitations) is compensated for the inclusive scattering making use of the dispersion relations. The larger cross sections in the RGF arise from the translation to the inclusive strength of the overall effects of inelastic channels. These contributions are not included

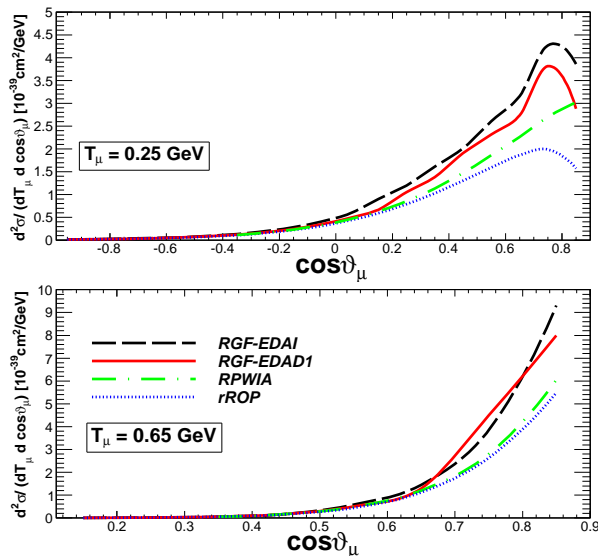


Figure 2. (color online) Flux-averaged double-differential cross section per target nucleon for the CCQE  $^{12}\text{C}(\bar{\nu}_\mu, \mu^+)$  reaction as a function of  $\cos\vartheta_\mu$  for two bins of  $T_\mu$  calculated with the RGF-EDAD1 (solid lines) and the RGF-EDAI (dashed lines). The dotted lines are the rROP results calculated with the EDAI potential and the dot-dashed lines are the RPWIA results.

explicitly in the RGF model, but can be recovered, at least to some extent, in the RGF by the imaginary part of the phenomenological optical potential which reincorporates these processes in the reaction.

In Fig. 2 the CCQE flux-averaged double-differential  $^{12}\text{C}(\bar{\nu}_\mu, \mu^+)$  cross section per target nucleon is displayed as a function of  $\cos\vartheta_\mu$  for two bins of  $T_\mu$ . Similar considerations can be made for these results: the rROP gives the lower results and the RGF cross sections with both optical potentials are larger than the RPWIA and the rROP ones. All the models, however, tend to produce similar results for backward scattering angles, where the cross sections are sensibly reduced. The differences between the RGF results with the two optical potentials are visible but they are somewhat reduced with respect to the corresponding calculations for neutrino scattering in Fig. 2 of Ref. [56]. This is essentially due to the combined effects of the differences between the  $\nu_\mu$  and the  $\bar{\nu}_\mu$  fluxes and of the destructive contribution of the vector-axial interference response.

In Fig. 3 the total QE cross sections per target nucleon for neutrino and antineutrino scattering are displayed as a function of the neutrino (antineutrino) energy  $E_\nu$  ( $E_{\bar{\nu}}$ ). The neutrino results, which have been already presented in Ref. [56], are compared with the experimental data from MiniBooNE [1]. In Refs. [27, 34] it is shown that DWIA models where FSI effects are accounted for by means of real potentials, like rROP and RMF, produce similar results which all underestimate the total CCQE

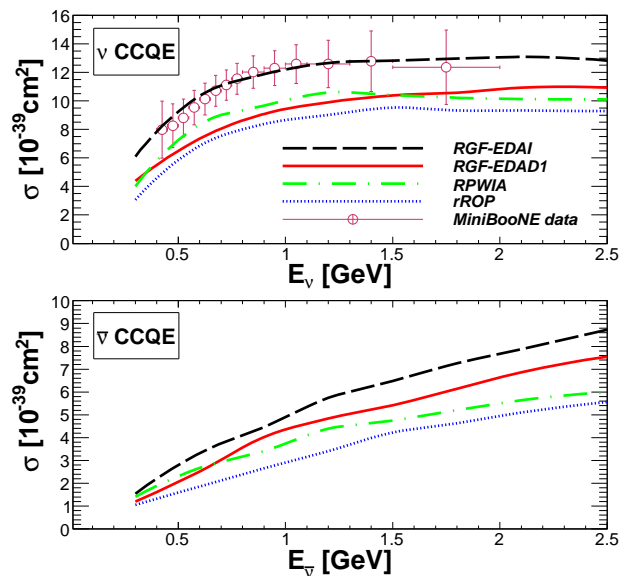


Figure 3. (color online) Total CCQE cross section per target nucleon as a function of the neutrino energy  $E_\nu$  (upper panel) and of the antineutrino energy  $E_{\bar{\nu}}$  (lower panel) calculated with the RGF-EDAD1 (solid lines), the RGF-EDAI (dashed lines), the rROP (dotted lines), and the RPWIA (dot-dashed lines). The experimental data for neutrino scattering are from MiniBooNE [1].

MiniBooNE cross section, whereas the inclusion of 2p-2h MEC enhances the results. Larger cross sections are obtained in the RGF with both optical potentials. The differences between RGF-EDAI and RGF-EDAD1 are clearly visible, RGF-EDAI being in good agreement with the shape and magnitude of the experimental cross section for neutrino scattering. We observe that EDAI is a single-nucleus parameterization, which is constructed to better reproduce the elastic proton- $^{12}\text{C}$  phenomenology, and gives electron scattering cross sections in fair agreement with the experimental data. We also note that the antineutrino cross section does not saturate in the energy range up to 2.5 GeV which we have considered. Also in this case, the differences between EDAI and EDAD1 are due to the different imaginary parts of the two potentials, particularly for the energies considered in kinematics with the largest  $T_\mu$ . These kinematics give large contributions to the total cross section and enhance the differences between the two RGF results.

### III. SUMMARY AND CONCLUSIONS

In this paper, we have compared the predictions of different relativistic descriptions of FSI for CCQE antineutrino-nucleus scattering in the MiniBooNE kinematics. In the RPWIA, FSI are simply neglected; in the rROP, they are described retaining only the real part of the relativistic energy-dependent optical potential; in the



RGF, the full complex optical potential, with its real and imaginary parts, is used to account for FSI. All final-state channels are included in the RGF, where the flux lost in each channel is recovered in the other channels by the imaginary part of the optical potential making use of the dispersion relations and the total flux is conserved. The RGF is able to give a good description of the  $(e, e')$  data in the QE region and it is also able to describe both the MiniBooNE CCQE and NCE neutrino data without the need to change the value of the axial mass.

The enhancement of the RGF cross sections compared to the cross sections calculated with other descriptions of FSI is obtained also in the case of antineutrino scattering. The larger results of the RGF can be ascribed to the contribution of reaction channels which are not included in the other models. For instance, rescattering processes of the nucleon in its way out of the nucleus, non-nucleonic  $\Delta$  excitations, which may arise during nucleon propagation, with or without real pion production, or also multinucleon processes. These contributions are not included explicitly in the RGF model, but can be recovered, to some extent, by the imaginary part of the phenomenological optical potential. We cannot disentangle the role of different reaction processes and explain in detail the origin of the recovered strength. It would be anyhow interesting for a comparison to disentangle in the phenomenological optical potential the contributions due to non-nucleonic inelasticities and extract a “purely nucleonic” optical potential that could be used in the RGF approach.

The RGF predictions are also affected by uncertainties in the determination of the phenomenological optical potential, which is not univocally determined from the elastic phenomenology. In the case of antineutrino scattering the differences between the RGF cross sections calculated with the EDAI and EDAD1 optical potentials are somewhat reduced with respect to the corresponding cross sections calculated for neutrino scattering. The differences between the RGF results for neutrino and antineutrino scattering may be ascribed to the different  $\nu_\mu$  and  $\bar{\nu}_\mu$  fluxes and to the strength of the vector-axial response. A better determination of the phenomenological relativistic optical potential, which closely fulfills the dis-

person relations, would reduce the theoretical uncertainties on the RGF results and, therefore, deserves further investigation.

The analysis of MiniBooNE CCQE and NCE data with theoretical models based on the IA and including only one-nucleon knockout contributions usually requires a larger value of  $M_A$  to reproduce the magnitude of the experimental cross sections. The calculations required for the theoretical analysis must consider the entire range of the relevant MiniBooNE neutrino energies and additional complications may arise from the flux-average procedure to evaluate the cross sections, which implies a convolution of the double-differential cross section over the neutrino spectrum. Because of uncertainties associated with the flux-average procedure, the MiniBooNE cross sections can include contributions from different kinematic regions, where other reaction mechanisms than one-nucleon knockout are known to be dominant [16, 17].

Models including other contributions than one-nucleon knockout, like our RGF, but also the model of Refs. [21–23], where multinucleon components are explicitly included, are able to describe the MiniBooNE neutrino data without the need to change the value of the axial mass. Despite their differences, the two models seem to go in the same direction. In the RGF, however, the enhancement of the cross section cannot be attributed only to multinucleon processes, since we cannot disentangle the role of the various contributions included in the phenomenological optical potential. In order to clarify this point a careful evaluation of all nuclear effects and of the relevance of multinucleon emission and of some non-nucleonic contributions would therefore be highly desirable.

## ACKNOWLEDGMENTS

We would like to thank J.A. Caballero and J. Grange for useful comments. This work was partially supported by the Italian MIUR through the PRIN 2009 research project.

- 
- [1] A. A. Aguilar-Arevalo *et al.* (MiniBooNE Collaboration), *Phys. Rev. D* **81**, 092005 (2010).
  - [2] A. A. Aguilar-Arevalo *et al.* (MiniBooNE Collaboration), *Phys. Rev. D* **82**, 092005 (2010).
  - [3] Y. Nakajima *et al.* (SciBooNE Collaboration), *Phys. Rev. D* **83**, 012005 (2011).
  - [4] R. Gran *et al.* (K2K Collaboration), *Phys. Rev. D* **74**, 052002 (2006), arXiv:hep-ex/0603034.
  - [5] Q. Wu *et al.* (NOMAD Collaboration), *Phys. Lett. B* **660**, 19 (2008).
  - [6] V. Lyubushkin *et al.* (NOMAD Collaboration), *Eur. Phys. J. C* **63**, 355 (2009).
  - [7] P. Adamson *et al.* (MINOS Collaboration), *Phys. Rev. D* **81**, 072002 (2010).
  - [8] D. Casper, *Nucl. Phys. Proc. Suppl.* **112**, 161 (2002), arXiv:hep-ph/0208030.
  - [9] Y. Hayato, *Nucl. Phys. Proc. Suppl.* **112**, 171 (2002).
  - [10] V. Bernard, L. Elouadrhiri, and U. G. Meissner, *J. Phys. G* **28**, R1 (2002), arXiv:hep-ph/0107088.
  - [11] A. Bodek, S. Avvakumov, R. Bradford, and H. Budd, *Eur. Phys. J. C* **53**, 349 (2008).
  - [12] B. Bhattacharya, R. J. Hill, and G. Paz, *Phys. Rev. D* **84**, 073006 (2011).
  - [13] A. Aguilar-Arevalo *et al.* (MiniBooNE Col-

- laboration), Phys.Rev. **D79**, 072002 (2009), arXiv:0806.1449 [hep-ex].
- [14] S. Boffi, C. Giusti, and F. D. Pacati, Phys. Rept. **226**, 1 (1993).
- [15] S. Boffi, C. Giusti, F. D. Pacati, and M. Radici, *Electromagnetic Response of Atomic Nuclei*, Oxford Studies in Nuclear Physics, Vol. 20 (Clarendon Press, Oxford, 1996).
- [16] O. Benhar, P. Coletti, and D. Meloni, Phys. Rev. Lett. **105**, 132301 (2010), arXiv:1006.4783 [nucl-th].
- [17] O. Benhar and G. Veneziano, Phys. Lett. B **702**, 433 (2011), arXiv:1103.0987 [nucl-th].
- [18] A. V. Butkevich, Phys. Rev. C **82**, 055501 (2010), arXiv:1006.1595 [nucl-th].
- [19] A. V. Butkevich and D. Perevalov, Phys. Rev. C **84**, 015501 (2011), arXiv:1106.0976 [hep-ph].
- [20] C. Juszczak, J. T. Sobczyk, and J. Zmuda, Phys. Rev. C **82**, 045502 (2010).
- [21] M. Martini, M. Ericson, G. Chanfray, and J. Marteau, Phys. Rev. C **80**, 065501 (2009), arXiv:0910.2622 [nucl-th].
- [22] M. Martini, M. Ericson, G. Chanfray, and J. Marteau, Phys. Rev. C **81**, 045502 (2010), arXiv:1002.4538 [hep-ph].
- [23] M. Martini, M. Ericson, and G. Chanfray, Phys. Rev. C **84**, 055502 (2011), arXiv:1110.0221 [nucl-th].
- [24] J. Nieves, I. Ruiz Simo, and M. J. Vicente Vacas, Phys. Rev. C **83**, 045501 (2011), arXiv:1102.2777 [hep-ph].
- [25] J. Nieves, I. Ruiz Simo, and M. J. Vicente Vacas, Physics Letters B **707**, 72 (2012), arXiv:1106.5374 [hep-ph].
- [26] J. E. Amaro, M. B. Barbaro, J. A. Caballero, T. W. Donnelly, and C. F. Williamson, Phys. Lett. B **696**, 151 (2011), arXiv:1010.1708 [nucl-th].
- [27] J. E. Amaro, M. B. Barbaro, J. A. Caballero, T. W. Donnelly, and J. M. Udías, Phys. Rev. D **84**, 033004 (2011), arXiv:1104.5446 [nucl-th].
- [28] A. Bodek, H. Budd, and M. Christy, Eur. Phys. J. C **71**, 1 (2011), arXiv:1106.0340 [hep-ph].
- [29] T. Leitner, O. Buss, L. Alvarez-Ruso, and U. Mosel, Phys. Rev. C **79**, 034601 (2009).
- [30] T. Leitner and U. Mosel, Phys. Rev. C **81**, 064614 (2010), arXiv:1004.4433 [nucl-th].
- [31] A. M. Ankowski and O. Benhar, Phys. Rev. C **83**, 054616 (2011).
- [32] E. Fernandez Martinez and D. Meloni, Physics Letters B **697**, 477 (2011).
- [33] A. De Pace, M. Nardi, W. M. Alberico, T. W. Donnelly, and A. Molinari, Nucl. Phys. **A726**, 303 (2003), arXiv:nucl-th/0304084 [nucl-th].
- [34] J. Amaro, M. Barbaro, J. Caballero, and T. Donnelly, Phys.Rev.Lett. **108**, 152501 (2012), arXiv:1112.2123 [nucl-th].
- [35] J. M. Udías, P. Sarriguren, E. Moya de Guerra, E. Garrido, and J. A. Caballero, Phys. Rev. C **48**, 2731 (1993), arXiv:nucl-th/9310004 [nucl-th].
- [36] J. M. Udías, P. Sarriguren, E. Moya de Guerra, E. Garrido, and J. A. Caballero, Phys. Rev. C **51**, 3246 (1995), arXiv:nucl-th/9312003 [nucl-th].
- [37] A. Meucci, C. Giusti, and F. D. Pacati, Phys. Rev. C **64**, 014604 (2001), arXiv:nucl-th/0101034 [nucl-th].
- [38] A. Meucci, Phys. Rev. C **65**, 044601 (2002), arXiv:nucl-th/0111077 [nucl-th].
- [39] M. Radici, A. Meucci, and W. H. Dickhoff, Eur. Phys. J. A **17**, 65 (2003).
- [40] T. Tamae, Y. Sato, T. Yokokawa, Y. Asano, M. Kawabata, O. Konno, I. Nakagawa, I. Nishikawa, K. Hirota, H. Yamazaki, R. Kimura, H. Miyase, H. Tsubota, C. Giusti, and A. Meucci, Phys. Rev. C **80**, 064601 (2009).
- [41] C. Giusti, A. Meucci, F. D. Pacati, G. Co', and V. De Donno, Phys. Rev. C **84**, 024615 (2011), arXiv:1105.1295 [nucl-th].
- [42] C. Maieron, M. C. Martinez, J. A. Caballero, and J. M. Udías, Phys. Rev. C **68**, 048501 (2003), arXiv:nucl-th/0303075 [nucl-th].
- [43] J. A. Caballero, Phys. Rev. C **74**, 015502 (2006), arXiv:nucl-th/0604020 [nucl-th].
- [44] J. A. Caballero, M. C. Martinez, J. L. Herreaz, and J. M. Udías, Phys. Lett. B **688**, 250 (2010), arXiv:0912.4356 [nucl-th].
- [45] A. Meucci, C. Giusti, and F. D. Pacati, Nucl. Phys. **A739**, 277 (2004), arXiv:nucl-th/0311081 [nucl-th].
- [46] A. Meucci, F. Capuzzi, C. Giusti, and F. D. Pacati, Phys. Rev. C **67**, 054601 (2003), arXiv:nucl-th/0301084 [nucl-th].
- [47] A. Meucci, C. Giusti, and F. D. Pacati, Nuclear Physics A **744**, 307 (2004), arXiv:nucl-th/0405004 [nucl-th].
- [48] A. Meucci, C. Giusti, and F. D. Pacati, Acta Phys. Polon. B **37**, 2279 (2006).
- [49] A. Meucci, C. Giusti, and F. D. Pacati, Nuclear Physics A **773**, 250 (2006), arXiv:nucl-th/0601052 [nucl-th].
- [50] A. Meucci, C. Giusti, and F. D. Pacati, Phys. Rev. C **77**, 034606 (2008).
- [51] A. Meucci, J. A. Caballero, C. Giusti, F. D. Pacati, and J. M. Udías, Phys. Rev. C **80**, 024605 (2009), arXiv:0906.2645 [nucl-th].
- [52] A. Meucci, J. A. Caballero, C. Giusti, and J. M. Udías, Phys. Rev. C **83**, 064614 (2011), arXiv:1103.0636 [nucl-th].
- [53] Y. Horikawa, F. Lenz, and N. C. Mukhopadhyay, Phys. Rev. C **22**, 1680 (1980).
- [54] F. Capuzzi, C. Giusti, and F. D. Pacati, Nuclear Physics A **524**, 681 (1991).
- [55] F. Capuzzi, C. Giusti, F. D. Pacati, and D. N. Kadrev, Annals of Physics (N.Y.) **317**, 492 (2005), arXiv:nucl-th/0410103 [nucl-th].
- [56] A. Meucci, M. B. Barbaro, J. A. Caballero, C. Giusti, and J. M. Udías, Phys. Rev. Lett. **107**, 172501 (2011), arXiv:1107.5145 [nucl-th].
- [57] A. Meucci, C. Giusti, and F. D. Pacati, Phys. Rev. D **84**, 113003 (2011), arXiv:1110.3928 [nucl-th].
- [58] A. A. Aguilar-Arevalo *et al.* (MiniBooNE Collaboration), Phys. Rev. D **84**, 072005 (2011).
- [59] <http://www-boone.fnal.gov>.
- [60] B. D. Serot and J. D. Walecka, Adv. Nucl. Phys. **16**, 1

- (1986).
- [61] M. M. Sharma, M. A. Nagarajan, and P. Ring, Phys. Lett. B **312**, 377 (1993).
- [62] G. A. Lalazissis, J. König, and P. Ring, Phys. Rev. C **55**, 540 (1997), arXiv:nucl-th/9607039 [nucl-th].
- [63] B. C. Clark, in *Proceedings of the Workshop on Relativistic Dynamics and Quark-Nuclear Physics*, edited by M. B. Johnson and A. Picklesimer (John Wiley & Sons, New York, 1986) p. 302.
- [64] E. D. Cooper, S. Hama, B. C. Clark, and R. L. Mercer, Phys. Rev. C **47**, 297 (1993).
- [65] E. D. Cooper, S. Hama, and B. C. Clark, Phys. Rev. C **80**, 034605 (2009).